Size-dependent photoabsorption and photoemission of small metal particles

W. Ekardt
Fritz-Haber-Institut der Max-Planck-Gesellschaft, Faradayweg 4-6, D-1000 Berlin 33, Germany
(Received 20 December 1984)

The dynamical electronic response properties of small metal particles are calculated within the frame of the self-consistent spherical jellium model. The method used is the TDLDA (time-dependent local-density approximation) with the inclusion of exchange and correlation. In this way we obtain for the first time insight into the nonlocal electronic response properties at a strictly microscopic level. The size dependence of photoabsorption, photoemission, and of the static polarizability, is discussed in detail. The emergence of the collective volume mode (the volume plasmon) as a function of the numbers of electrons is shown here for the first time. Likewise, the size-dependent Landau damping of these modes is obtained in a quantitative fashion. Compared with the results of any non-self-consistent model, we conclude that only a self-consistent theory like the TDLDA (or an improvement of it) is able to account for all the complexity of the electronic response in small dimensions.

I. INTRODUCTION

In recent years, the physics of small metal particles[1] has attracted much interest mainly for two reasons: On one hand this is an interesting field of research *per se* because the physical properties as a function of size are expected to show a more or less smooth transition from atomiclike behavior to solid-state-like features. On the other hand, small metal particles are of technological importance for the wide field of the heterogeneous catalysis and for this reason size-selective chemical properties (like cluster chemisorption) are of special interest.

Whereas the ground-state properties of clusters such as the cohesive energy, adhesive energy, and chemisorption energy can now be obtained at a microscopic level (if the number of atoms is not too large)[2] the situation is much worse as far as the dynamical properties are concerned. The reason for this is twofold. First, for the excited states of a system, a simple calculational scheme such as the local-density approximation (LDA) for the ground state does not exist. Second, we always need to know the complete spectrum instead of just one state (for the description of the ground state) to learn something on the dynamics of the system. It is mainly for these reasons that nearly nothing is known, at a strictly microscopic level, about the dynamical properties of aggregates consisting of more than two atoms.

However, quite recently it was experimentally confirmed by Knight *et al.*[3,4] that theoretical predictions based on a relatively simple model, namely the spherical jellium particle,[5–7] reproduce well part of the experimental observations concerning the ground state of small clusters of the light metals of Na and K. Even more recently Knight *et al.*[8] were able to show that the theoretically predicted size dependence of the static polarizability as calculated within a self-consistent spherical jellium model[9–11] agrees well with the experimental data on Na. Hence, it is both tempting and promising to extend this model to the description of the *dynamical* behavior of small metal particles. First results of this method were already published elsewhere,[9] and it is the aim of the present work to present the results in more detail and to extend the method to photoemission. It is hoped that (as it was the case with the *static* polarizability) at least for the light metals such as Na there is some relevance of the model description for the dynamical behavior of the loosely bound valence electrons.

II. THEORY

If the metal particle is placed in an oscillatory external potential $V_{\rm ex}(\mathbf{r};\omega)e^{-i\omega t}$, an induced electronic charge density is set up which is given by (within *linear*-response theory and with neglect of retardation)[12]

$$\rho_{\rm ind}(\mathbf{r},\omega)=\int d\mathbf{r}'\,\chi(\mathbf{r},\mathbf{r}';\omega)V_{\rm ex}(\mathbf{r}';\omega)\ . \tag{1}$$

In this equation $\chi(\mathbf{r},\mathbf{r}';\omega)$ is the dynamical density-density correlation function.

An exact determination of χ is impossible, of course. However, for *both* metal surfaces[13] *and* for atoms[14,15] and molecules[16,17] it has been shown that the so-called time-dependent LDA (TDLDA)[14] seems to reproduce most of the experimental data very well.[18]

Within the TDLDA, which has the same structure as the random-phase approximation with exchange,[19,20] the density-density correlation function is determined by the following integral equation:

$$\chi(\mathbf{r},\mathbf{r}';\omega)=\chi^0(\mathbf{r},\mathbf{r}';\omega)+\int\int d\mathbf{r}''\,d\mathbf{r}'''\,\chi^0(\mathbf{r},\mathbf{r}'';\omega)K(\mathbf{r}'',\mathbf{r}''')\times\chi(\mathbf{r}''',\mathbf{r}';\omega)\ . \tag{2}$$

This equation results from the self-consistency condition of the independent-particle response to the total effective potential $V_{\rm eff}(\mathbf{r};\omega)$ in the following way:

$$\rho_{\rm ind}(\mathbf{r},\omega)=\int d\mathbf{r}'\,\chi^0(\mathbf{r},\mathbf{r}';\omega)V_{\rm eff}(\mathbf{r}',\omega)\ , \tag{3}$$

$$V_{\rm eff}(\mathbf{r},\omega)=V_{\rm ex}(\mathbf{r},\omega)+\int d\mathbf{r}'\,K(\mathbf{r},\mathbf{r}')\rho_{\rm ind}(\mathbf{r}',\omega)\ . \quad (4)$$

In these equations $\chi^0(\mathbf{r},\mathbf{r}';\omega)$ is the independent particle density-density correlation function and the kernel $K(\mathbf{r},\mathbf{r}')$ is given by

$$K(\mathbf{r},\mathbf{r}')=\frac{2}{|\mathbf{r}-\mathbf{r}'|}+\frac{dV_{\rm xc}}{d\rho}\delta(\mathbf{r}-\mathbf{r}')\ . \quad (5)$$

In Eq. (5), $dV_{\rm xc}/d\rho$ is the density derivative of the exchange-correlation potential in the ground state and the independent-particle density-density correlation function is given by[14]

$$\chi^0(\mathbf{r},\mathbf{r}';\omega)=\sum_i^{\rm occ}\phi_i^*(\mathbf{r})\phi_i(\mathbf{r}')G(\mathbf{r},\mathbf{r}';\epsilon_i+\hbar\omega)+\sum_i^{\rm occ}\phi_i(\mathbf{r})\phi_i^*(\mathbf{r}')G^*(\mathbf{r},\mathbf{r}';\epsilon_i-\hbar\omega)\ . \quad (6)$$

In Eq. (6) the sum is over all occupied states $\{i\}$ in the ground-state and G is the retarded Green's function of the ground state Hamiltonian. Within the TDLDA the single-particle wave functions ϕ_i are assumed to be given to a good approximation by the Kohn-Sham orbitals in the ground state, and this assumption is an unproven step in the formalism. However, experience has shown that this seems to be a quite good (or excellent) approximation for the description of the dynamical response of the *loosely bound* valence electrons of atoms, molecules, and solid surfaces. Thus it seems reasonable to expect that this approximation also works quite well in the case of atomic aggregates. The physical content of the formalism described so far is that of all the many-particle effects the important dielectric effects are fully included whereas relaxation effects are completely neglected (however, see Ref. 18). Thus if one wants to study the evolution of collective effects like plasmons etc. the formalism seems to be quite adequate.

A prerequisite of the TDLDA ia the knowledge of the "Kohn-Sham ground state" of the system and these calculations were already performed[6,7,11] for the spherical jellium particle. Hence, we are ready to solve for the response equations.

Due to the spherical nature of the system, the equations considerably simplify for completely filled shells in the ground state since, in this case, the response is diagonal with respect to the angular momentum L of the external perturbation $V_{\rm ex}$.[14] In this paper we are exclusively concerned with the dipole response properties. Therefore we need to specialize the response equations to the case $L=1$. These special equations were already published in Ref. 9 and they are only shortly reproduced here. If an angular representation is used for all quantities, Eq. (2) simplifies to

$$\chi_l(r,r';\omega)=\chi_l^0(r,r';\omega)+\int_0^\infty dr''(r'')^2\chi_l^0(r,r'';\omega)[dV_{\rm xc}/d\rho]\chi_l(r'',r';\omega)+\int_0^\infty dr'''(r''')^2\int_0^\infty dr''r''^2\chi_l(r,r'';\omega)[4\pi/(2l+1)]B_l(r'',r''')\chi_l(r''',r';\omega)\ , \quad (7)$$

where we have introduced $B_l(x,y)=2x_<^l/y_>^{l+1}$ and χ_l^0 is the lth component of the independent particle susceptibility. As was shown by Zangwill and Soven (see also Ref. 21) this quantity is given by (for $L=1$)

$$\chi_1^0(r,r';\omega)=\sum_{l,n_l}^{\rm occ}(1/2\pi)R_{l,n_l}(r)R_{l,n_l}(r')[(l+1)G_{l+1}(r,r';\epsilon_{l,n_l}+\omega)+lG_{l-1}(r,r';\epsilon_{l,n_l}+\omega)+(l+1)G_{l+1}^*(r,r';\epsilon_{l,n_l}-\omega)+lG_{l-1}^*(r,r';\epsilon_{l,n_l}-\omega)]\ . \quad (8)$$

In Eq. (8), $R_{l,n_l}(r)$ is the radial part of the occupied state $\{l,n_l\}$ in the ground state with energy ϵ_{l,n_l}, ω is the frequency of the external photon, and the Green's function $G_l(r,r';E)$ is obtained by two solutions of the ground-state Schrödinger equation in the following way:[14]

$$G_l(r,r';E)=\frac{j_l(r_<;E)h_l(r_>;E)}{\{r^2W(j_l;h_l)\}_{r=c}}\ . \quad (9)$$

In this equation j_l is regular at the origin, h_l fulfills the outgoing-wave boundary condition, W is the Wronskian, and c is an arbitrary constant. Having obtained $\chi_1(r,r';\omega)$ we are ready to calculate every physical quantity which is characteristic to the linear dipole response of the small metal particle.

III. STATIC POLARIZABILITY

Once $\chi_1(r,r';\omega)$ is known the complex induced charge density and the complex polarizability $\alpha(\omega)$ are given as follows:[9]

$$\rho_{\rm ind}(\mathbf{r},\omega)=-(4\pi/3)^{1/2}y_{1,0}(\theta)E_0\times\left[2\int_0^\infty dr'\chi_1(r,r';\omega)(r')^3\right]\ , \quad (10)$$

$$\alpha(\omega)=\int_0^\infty dr\,r\alpha(r,\omega)\ , \quad (11)$$

$$\alpha(r,\omega)=-(4\pi/3)r^2 2\int_0^\infty dr'\chi_1(r,r';\omega)r'^3\ . \quad (12)$$

To obtain the static dielectric behavior we have to solve Eq. (2) and to calculate Eqs. (10)—(12) for $\omega=0$.

In Fig. 1 the dots show the static polarizability $\alpha(0)$, in units of its classical value $\alpha_{\rm cl}=R^3$, for the various completely filled shells of a small jellium sphere corresponding to sodium. R is the particle radius related to the number of particles via $R=r_sN^{1/3}$. The result is compared with the polarizability obtained from various non-self-consistent theories like the quantum infinite-barrier model,[22] the semiclassical infinite-barrier model,[23] or the step-density modified Thomas-Fermi approximation.[24] In sharp contrast to the results of these models the self-consistently obtained polarizability per atom of a Kohn-

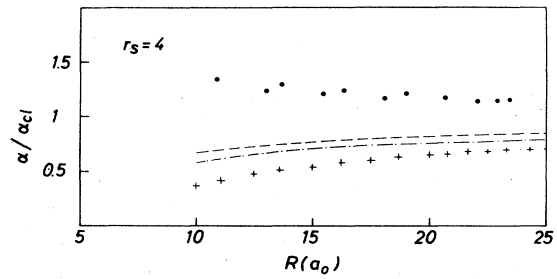

FIG. 1. Static polarizability α of a small jellium sphere for $r_s=4$, corresponding to the bulk density of Na, in units of its classical value, $\alpha_{cl}=R^3$, as a function of its size. R is the jellium background radius, $R=r_sN^{1/3}$, in a.u. Dots, present theory; dashed line, step-density Thomas-Fermi approximation, Ref. 24; dashed-dotted line, semiclassical approximation, Ref. 23; crosses, quantum infinite-barrier model, Ref. 22.

Sham sphere does not decrease but increases weakly if the number of atoms within the particle goes down! In addition the size effect within the TDLDA is much weaker than in any non-self-consistent theory. The microscopic reason for this behavior can be seen from Fig. 2, which shows the (normalized) polarization charge density,

$$\tilde{\alpha}(r;0)\equiv\alpha(r;0)\Big/\int_0^\infty dr\,\alpha(r;0)\ ,$$

for four different particle numbers. There are two striking features. First, the big hump across the jellium surface shows only a very weak size dependence. Second, the $\tilde{\alpha}(r;0)$ across the surface looks very similar to the normalized induced charge density at a planar jellium surface.[25] Consequently the location of the static apparent image sphere δ, defined as $\alpha=(R+\delta)^3$, is very similar to the location of the planar image plane. For instance, the values of δ for the completely filled s shells $2s$, $3s$, and $4s$, corresponding to particle numbers 20, 92, and 198, respectively, are given by $\delta_{2s}=1.098$, $\delta_{3s}=1.035$, $\delta_{4s}=1.182$ a.u. Whereas the value for the semi-infinite half-space[25] is $\delta_\infty=1.3$ a.u. Having no strictly monotonous behavior of δ relates to the quantum size effects in small metal particles.

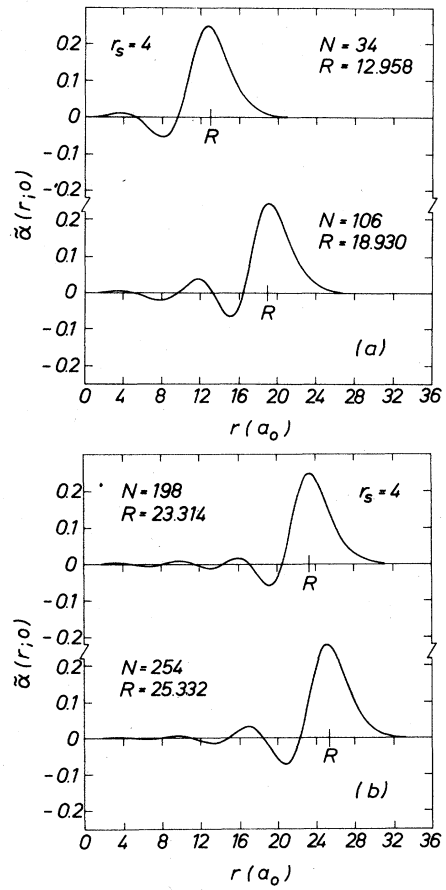

FIG. 2. Evolution of the normalized polarization charge density as a function of size. The striking feature here is that $\alpha(r;0)$ across the surface looks very similar to the corresponding value at a planar jellium surface. As a consequence, the location of the apparent image sphere is similar to the location of the image plane. For a detailed discussion see text.

The microscopic origin of why α/α_{cl} is always larger than 1 relates to the fact that, due to the diffuse nature of the electronic ground-state density,[6,7] the induced charge resides partly *outside* the classical surface of the particle. In all the other models[22–24] this relaxation is toward the *interior* of the particle which makes the polarizability smaller than its classical value R^3.

Quite recently[4,8] this behavior has been experimentally confirmed. The static polarizability per atom of small clusters of Na in the gas phase is a *weak* size-dependent quantity and decreases if the number of atoms is enlarged. This is exactly the behavior shown by the dots in Fig. 1. Furthermore, because the magic numbers found by Knight *et al.* agree with those of the spherical jellium model we conclude that the originally made assumption[6] concerning the usefulness of the self-consistent spherical jellium model is approximately fulfilled, at least for the light metals like Na and K.

To conclude this section we show in Fig. 3 the radial component of the total self-consistent potential $V_{\rm eff}=V_{\rm ex}+V_{\rm ind}$ and the radial component of the electrostatic field across the particle.[26] Two striking features are: (1) $V_{\rm eff}(r=R)$ is approximately zero, and (2) the electrostatic field across the surface is very similar to the one obtained for a semi-infinite half-space. The approximate vanishing of the *total* effective potential is due to the electrostatic force sum rule[27,28] which means physically that the particle does not move under the influence of a homogeneous electrostatic field. This means that the total *electrostatic* part of the potential at the jellium edge equals zero. A mathematical convenient form of this statement, namely[9]

$$1=-(4\pi/3)\int_0^R dr\,(r/R)^3\int_0^\infty dr'2\chi_1(r,r';0)r'^3 -(4\pi/3)\int_R^\infty dr\int_0^\infty dr'2\chi_1(r,r';0)r'^3\ , \qquad (13)$$

has been used as a check on the numerical work.[9] Typically, Eq. (13) is fulfilled to within a relative accuracy of 10^{-4}.

Finally, we want to compare our results with similar work of Refs. 10, 11, and 28. The results of Ref. 10 and the present work should be nearly identical (for $r_s=4$) and

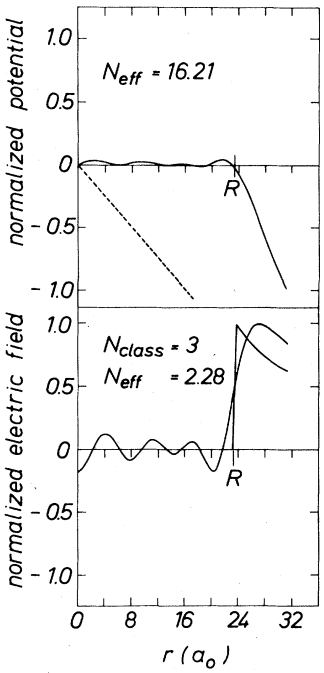

FIG. 3. Radial part of the total effective potential and radial part of the radial component of the electrostatic field for $r_s=4$, $N=198$, and $\omega=0$. Both quantities are "normalized to one," which means they are to be multiplied with the numbers given in the figure as $N_{\rm class}=198$ and $N_{\rm eff}=254$. The dashed-dotted line in the upper part gives the external potential $V_{\rm ex}=-r$. Due to the electrostatic force sum rule the electrostatic part of $V_{\rm eff}$ at $r=R$ is equal to zero. The behavior of the electrostatic field across the surface is similar to that at a planar jellium surface, recently discussed by Andersson *et al.* (Ref. 26). The classic electrostatic field is also shown for comparison. The classical zero field inside the particle can roughly be understood as the macroscopic average of the microscopic quantum oscillations.

indeed they are (more or less). *Small* differences can be caused by the use of a different approximation for the description of correlation and, may be, due to different numerical details. The results of Ref. 11 are similar, however a *direct* comparison is not possible, simply because no results are given there for $r_s=4$.

The results obtained within a statistical treatment of the kinetic energy of the electrons[28] agree more or less with the present ones. Hence, we think that the problem of the static polarizability is basically solved.

Before we continue with a discussion of the dynamical response, we shortly comment on the static polarizability of *embedded* clusters compared to their classical value, which is known to be given by $R^3(\epsilon-\epsilon_d)/(\epsilon+2\epsilon_d)$, with ϵ_d the static dielectric constant of the embedding host. As we have seen above, in a self-consistent-field (SCF)-like theory, the induced charge density is mainly determined by the electronic ground state profile across the surface. Hence if, due to strong repulsive forces, the embedding leads to a steeper electronic profile a reduction of the static polarizability is to be expected. If, on the other hand, the density profile upon embedding looks softer an *enlarged* polarizability will be the consequence. Both kinds of this behavior seem to have been observed experimentally, as we shall see later.

IV. PHOTOABSORPTION

If Eq. (2) is solved for a variable frequency ω, the dynamical polarizability and the induced polarization density are obtained via Eqs. (11) and (12). With the help of this, $\alpha(\omega)$, the cross section for photoabsorption is given by $\sigma(\omega)=4\pi(\omega/c)\mathrm{Im}\alpha(\omega)$.[14] Hence, the important quantity is the imaginary part of $\alpha(\omega)$.

In the classical theory of local optics the frequency-dependent polarizability $\alpha(\omega)$ of a metal sphere of radius R and with a local bulk dielectric constant $\epsilon(\omega)$ is given by

$$\alpha^{\rm cl}(\omega)=R^3\frac{\epsilon(\omega)-1}{\epsilon(\omega)+2}\ . \tag{14}$$

If the Drude dielectric constant is used to calculate $\alpha^{\rm cl}(\omega)$, the dynamical response is governed exclusively by the classical Mie resonance of the particle which peaks at $\omega_p/\sqrt{3}$. The imaginary part of $\alpha(\omega)$ in this case is given by

$$\mathrm{Im}[\alpha(\omega)]/R^3=\Omega\Gamma/[(1-\Omega)^2+\Gamma^2\Omega^2]\ , \tag{15}$$

with $\Omega=\omega/(\omega_p/\sqrt{3})$ and $\Gamma=\delta/(\omega_p/\sqrt{3})$, where δ is the damping of the single particle states in the Drude dielectric constant. A resulting Drude-absorption spectrum for small damping ($\delta=10$ meV) is given, for instance, by the continuous line in Figs. 4–6.

Quantum mechanically, we expect the following general equation to be valid instead of Eq. (14):

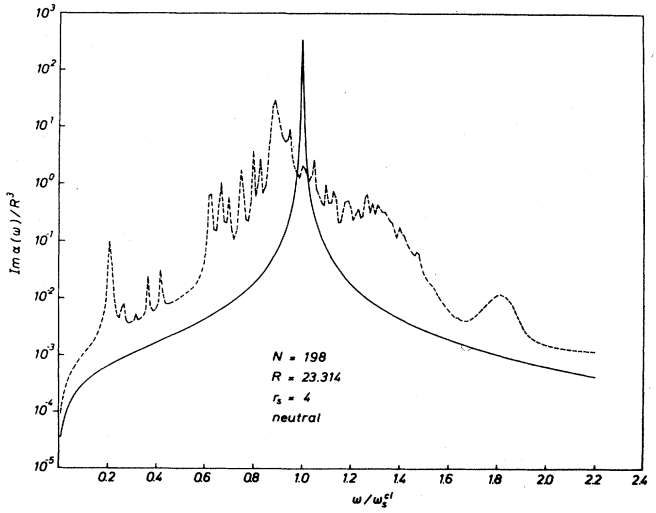

FIG. 4. Imaginary part of the dynamical polarizability, in units of R^3, for $r_s=4$ and $N=198$. The frequency ω is scaled with $\omega_s^{\rm cl}=\omega_p/\sqrt{3}$. The classical Drude result, the solid line, is also shown for comparison. The various fine cusps correspond to the excitation of single-particle-hole pairs, the large hump around 1.8 is the Landau-damped volume plasmon, and the central feature around 0.9 is the red-shifted Mie resonance of the particle. In sharp contrast to classical optics, due to the nonlocal nature of the electronic response the volume plasmon can be excited by photons.

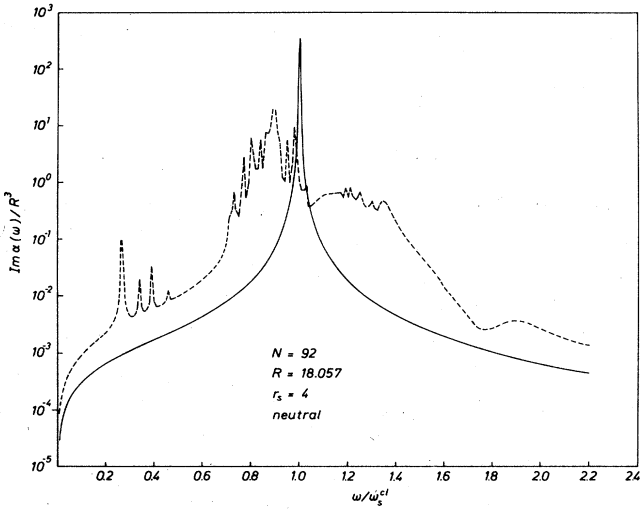

FIG. 5. The same as Fig. 4, but for $N=92$. The size-dependence of the quantum size effects can clearly be seen. Note that, compared to $N=198$, the volume plasmon around 1.9 is further blue shifted and starts disappearing. This is nothing else than *increased* Landau damping of the collective mode.

$$\alpha(\omega)=R^3\beta(\omega;R,r_s)\ , \tag{16}$$

where the factor β shows structure due to:

(i) The excitation of single electron hole pairs.

(ii) The excitation of collective volume modes (the plasmon whose optical excitation is forbidden within local electrodynamics).

(iii) The excitation of the quantum-mechanical analog to the classical Mie resonance.

Due to the quantum size effect and due to the changing volume to surface ratio all these features can be expected to be both size dependent and density dependent.

This is verified in Figs. 4—6, which show the imaginary part of $\alpha(\omega)$ for "sodium spheres" ($r_s=4$) of $N=198$, 92, and 20 valence electrons. These numbers correspond to completely filled $4s$, $3s$, and $2s$ shells, respectively. Compared to the size-independent continuous line there are several striking features. First, the surface-plasmon peak position is red shifted compared to its classical value $\omega_p/\sqrt{3}$. Second, this mode shows—compared to the classical curve—additional damping which obviously means that the collective mode decays in electron-hole pairs.

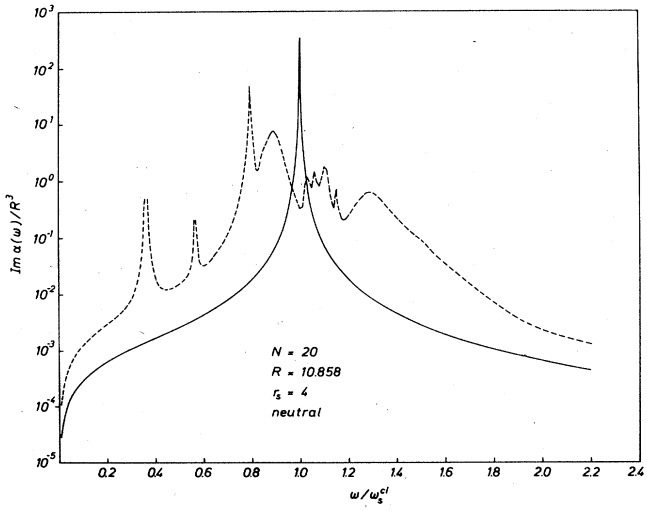

FIG. 6. The same as Fig. 4, but for $N=20$, now, the volume plasmon has disappeared.

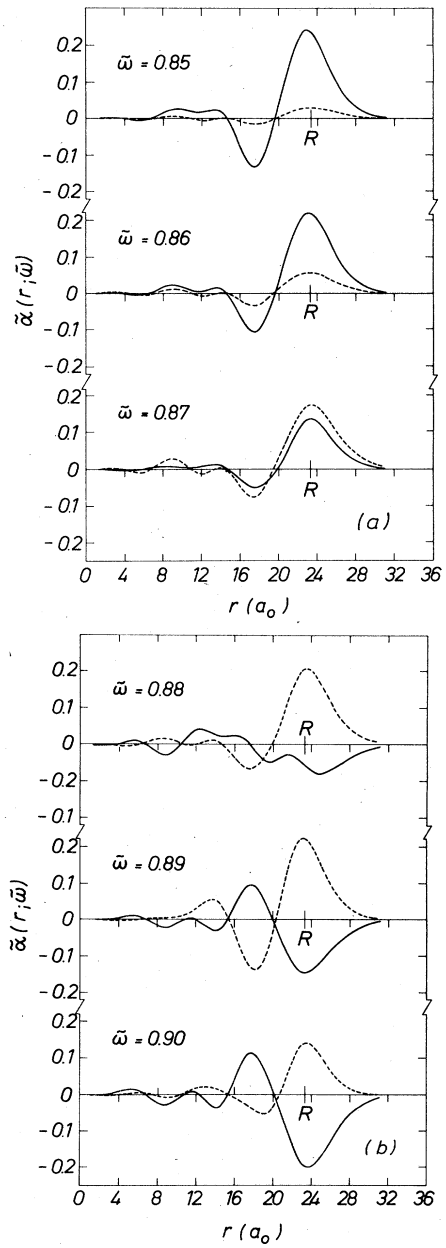

FIG. 7. Dynamically induced polarization charge density, $\tilde{\alpha}(r,\omega)=\alpha(r,\omega)/\left|\int_0^\infty dr\alpha(r,\omega)\right|$, where $\alpha(r,\omega)$ is defined by Eq. (12) of the text, for frequencies $\tilde{\omega}\equiv\omega/\omega_s^{cl}$ around the Mie resonance. Solid line, real part; dashed line, imaginary part. The exact location of the surface resonance is where the phase switch from 0 to π of the real part of $\alpha(r,\omega)$ occurs in the surface region.

This is nothing else than size-dependent Landau damping. Third, there is a size-dependent feature around the classical plasmon frequency ω_p, which is—compared to ω_p—blue shifted. This blue shift is the stronger the smaller the particle is. Fourth, this mode is considerably Landau damped and, for $N=20$, has eventually been destroyed. Fifth, there are additional narrow cusps in $\mathrm{Im}\alpha(\omega)$ which, obviously, correspond to the direct excitation of particle-hole pairs. The size dependence of all these features is more or less well pronounced. Hence, we see clearly that the use of an $\epsilon(\omega)$ certainly does not make sense.

The fact that the particle-hole lines are not δ functions is due to having used a complex photon frequency $\omega+i\delta$ with $\delta=10$ meV (for numerical convenience) instead of $\omega+i0^+$ in solving Eq. (2). Hence each particle-hole line has this "intrinsic numerical damping." Furthermore, every particle-hole line being located in the particle-hole continuum of any other bound-continuum transition region will get additional damping for exactly the same reason why the collective modes are decaying via size-dependent Landau damping. This damping is present for every bound-bound transition with a frequency above the first bound-continuum threshold. These transitions are nothing else but the well-known autoionization resonances of atomic and molecular physics.

The physical character of a certain excitation as being a single-pair or a collective surface mode or, virtually, a strong coupling between all these excitations can be visualized by looking at the frequency-dependent complex polarization charge density $\alpha(r,\omega)$. This is shown in Figs. 7–9. Figure 7 shows the *normalized* quantity $\tilde{\alpha}(r,\omega) \equiv \alpha(r,\omega)/\left|\int_0^\infty dr\alpha(r,\omega)\right|$, for frequencies ω around the large maximum in Fig. 4. We see that the imaginary part of $\alpha(r,\omega)$ (from which the absorption is calculated) grows up in the surface region whereas the real part (the continuous line in the figure) undergoes a phase switch by π. This is the typical behavior of a driven "surface oscillator." In the light of these remarks the large surface hump at $\omega=0$ (see Fig. 2) is nothing else than the *virtual* excitation of the surface plasmon.

The next figure (Fig. 8) shows the same phenomenon for a single-pair transition, namely for frequencies around the first spike in Fig. 4. The imaginary part of α is switched on at $\omega\approx 0.2\omega_p$ and is quickly switched off at $\omega=0.23\omega_p$. A careful line-shape analysis shows that the full width at half maximum agrees with what has been put in numerically. The phase switch from 0 to π of the real part takes place in the interior of the sphere *but not in the surface region.* There is only a small distortion of the surface charge density at resonance and this tells us that it does make sense to speak of single pairs and collective modes (despite the fact that all things are coupled together).

This simple picture changes if the particle number decreases. For $N=20$ the collective *volume* mode has already disappeared (see Fig. 6) and the dynamical charge density around the collective surface mode is quite complex. Figure 9 shows the real and imaginary part of $\alpha(r,\omega)$ for $0.75<\omega/\omega_s^{\mathrm{cl}}0.91$ which means, around the large cusp and the large hump of Fig. 6. Both the real and the imaginary part of $\alpha(r,\omega)$ are strongly distorted

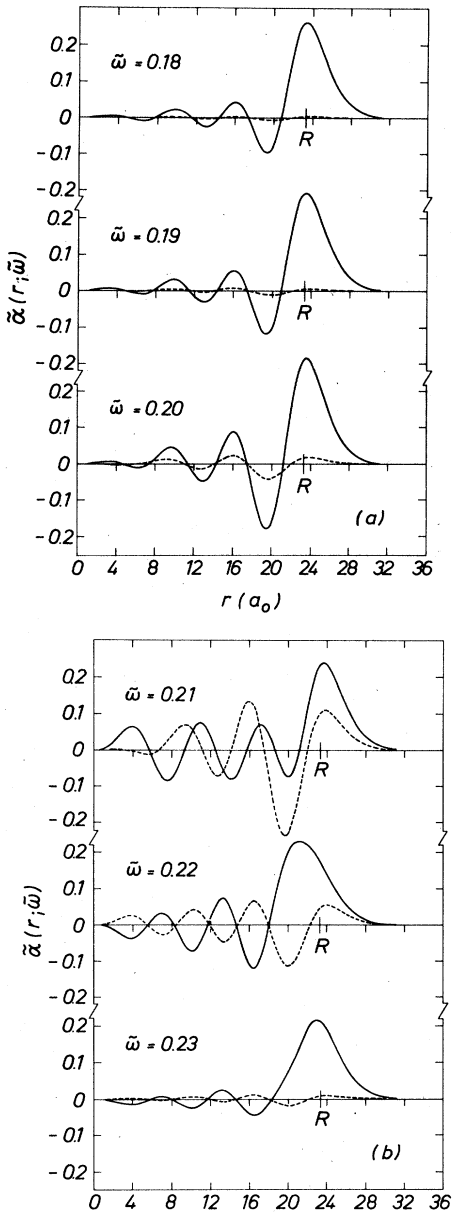

FIG. 8. The same as Fig. 7, but for the first particle-hole-pair transition (see Fig. 4). Here, the phase switch occurs in the *interior* of the sphere between $0.20\leq\tilde{\omega}\leq 0.22$. The charge density in the surface region is only slightly distorted. This tells us that it *does* make sense to speak of a single pair, simply because its coupling to the collective mode is small.

both in the volume region of the particle and across the surface. From these figures we conclude that most probably the term "single-pair" or "collective mode" starts losing its meaning.

On the other hand for larger particles, e.g., $N=198$, this terminology does make sense and we continue to comment on an approximation which has been termed in the past "surface-plasmon-pole approximation."[24] Under the assumption that all the optical oscillator strength is stored in just one collective pole, namely the surface-

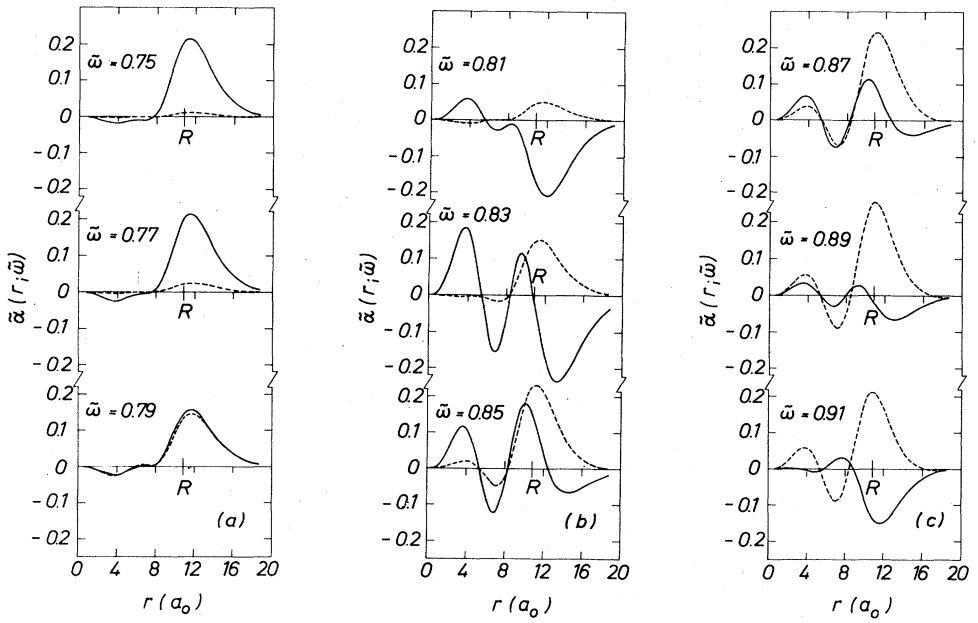

FIG. 9. The same as Fig. 7, but for $N=20$, in the frequency range $0.75 \leq \tilde{\omega} \leq 0.91$. For this small number of electrons, the surface mode is not as good decoupled from the interior of the sphere as it was the case for $N=198$ (see Fig. 7). Hence, all "oscillators" are strongly coupled together. Another consequence of this strong-coupling case is the disappearance of the volume plasmon as a well-defined collective excitation.

plasmon pole, one can show that its peak position is given by[24,29]

$$\omega^{\text{pole}} \Big/ \frac{\omega_p}{\sqrt{3}} = 1/\sqrt{\alpha(\omega=0)/R^3} \,. \tag{17}$$

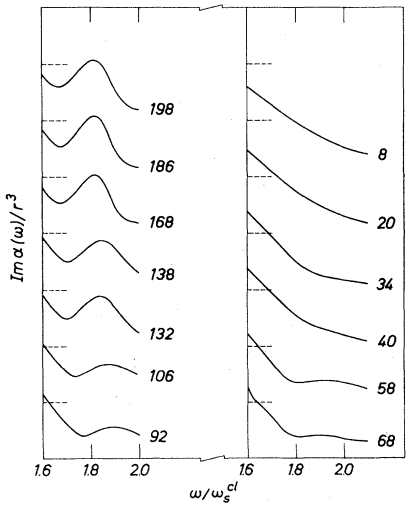

FIG. 10. $\mathrm{Im}\alpha(\omega)/R^3$ for various completely filled shells for N between 8 and 198 in a frequency range around the volume plasmon frequency. This figure shows explicitly how the plasmon emerges if the number of electrons increases. Every horizontal bar corresponds to the beginning of a logarithmic scale at 10^{-3}, belonging to the curve above this bar.

If we put in the values for $\alpha(\omega=0)$ and R pertaining to $N=198$, namely $\alpha(0)/R^3=1.16$ we get $\omega^{\text{pole}}/(\omega_p/\sqrt{3})=0.93$ compared to 0.88 from the exact calculation. Hence, the surface-plasmon-pole approximation is not so bad to get a first information on the collective pole. The advantage of this "method" is obvious: The only thing we need to know is the *static* polarizability which is much easier to obtain than the complete dynamical results.

To conclude this section we show in Fig. 10 the line shape of the collective volume mode (the plasmon) for spheres with uppermost filled shells of symmetry: $4S$ ($N=198$), $2G$ (186), $1J$ (168), $3P$ (138), $1I$ (132), $2F$ (106), $3S$ (92), $1H$ (90), $2D$ (68), $1G$ (58), $2P$ (40), $1F$ (34), $2S$ (20), and $1P$ (8).

We comment now on the microscopic origin for the blue or red shift of the collective frequencies compared to their classical counterparts $\omega_p/\sqrt{3}$ and ω_p. Obviously a diffuse surface profile makes all the collective frequencies softer, simply because the local reference point of the frequency goes down. On the other hand, the level quantization of the single-particle levels certainly leads to a blue shift, simply because the coupled oscillators are replaced with those of a "stiffer" force constant. Hence, there are two competing effects: The blue-shift level quantization and the red-shift surface diffuseness. Which effect will dominate, cannot be answered *a priori*. Obviously (but not surprisingly) the surface diffuseness dominates the surface mode whereas the level quantization dominates the volume mode. The reason why, for instance, the static

polarizability of the particle calculated in a completely self-consistent theory shows only a minor additional size effect (see Fig. 2) seems to relate to the competition between these two effects.

Finally it is only fair to say that Appell was the first (to the best of my knowledge) who predicted a red shift of the surface mode on the basis of an asymptotic expansion of the optical response of the sphere to account for the diffuse surface profile of the electronic charge.[30–34] However, he never gave *numerical* results and my own calculation of his definition of d_r/R yields, on the basis of the Kohn-Sham (KS) results, rather strange results. Here, d_r is the quantity δ we have discussed above. So it remains doubtful whether or not his formulation of the problem gives useful results (at least for larger spherical objects).

V. PHOTOEMISSION

On the experimental side both the enormously enhanced photo yield of small Ag particles[35] and the giant van der Waals forces between them[36] gave an important impact for the theoretical investigation of whether, and if so why, small metal particles show so radically different response properties when compared with a planar semi-infinite half-space. Quite recently, the same authors found that contamination of rest gas seems to play an important role.[37] As we shall see later in this section there is possibly a natural explanation for this experimental finding.

Within the TDLDA, the photoemission cross section from a bound level $\{n_l,l,m,s\}$ to the continuum of states $\{k',l',m',s'\}$ is given as follows:[14,15]

$$\sigma_{l,n_l}(\omega)=4\pi^2\frac{e^2}{\hbar c}\hbar\omega\sum_{k',l',m',s'}f_{n,l,m,s}(1-f_{k',l'm's'})\sum_{m,s}|\langle k',l',m's'|V_{\rm SCF}(\mathbf{r},\omega)|n_l,l,m,s\rangle|^2\delta(\hbar\omega+\epsilon_{n_l,l}-\epsilon_{k'})\ . \tag{18}$$

In this equation the single-particle states are to be calculated with the help of the single-particle ground-state potential[6,7] and the self-consistently determined driving potential for photoemission $V_{\rm SCF}$ is given within linear-response theory by

$$V_{\rm SCF}(\mathbf{r},\omega)=-\left[\frac{4\pi}{3}\right]^{1/2}y_{1,0}(\theta)\left[r+r\frac{4\pi}{3}\int_0^r dr'\left[\frac{r'}{r}\right]^3\int_0^\infty dr''(r'')^2 2\chi_1(r',r'';\omega)\right.$$
$$\left.+\int_r^\infty dr'\int_0^\infty dr''(r'')^2[2\chi_1(r',r'';\omega)]+V_{\rm xc}(r)\int_0^\infty dr'(r')^3\chi_1(r,r';\omega)\right]\ . \tag{19}$$

Here, $V_{\rm xc}(r)$ is the density-derivative of the exchange-correlation potential in the ground state[6] and $\chi_1(r,r';\omega)$ has been discussed above.

Inserting the expression for $V_{\rm SCF}(\mathbf{r},\omega)$, Eq. (19), in the matrix element, Eq. (18), and summing over all occupied states $\{n_l,l,m,s\}$ leads to the following expression for the *total* photoemission cross section $\sigma(\omega)$ (after spin and angular integration, respectively):

$$\sigma(\omega)=\frac{4\pi^2}{3}\frac{e^2}{\hbar c}\hbar\omega(\hbar\omega+\epsilon_{n_l,l})^{-1/2}$$
$$\times\sum_{n_l,l}^{\rm occ}[(l+1)|\langle k',l+1|V_{\rm SCF}(r,\omega)|n_l,l\rangle|^2+l|\langle k',l-1|V_{\rm SCF}(r,\omega)|n_l,l\rangle|^2]\theta(\hbar\omega+\epsilon_{n_l,l})\ . \tag{20}$$

In this equation, $V_{\rm SCF}(r,\omega)$ is the radial part of the self-consistent potential, Eq. (19), $\{n_l,l\}$ and $\{k',l'\}$ are the radial parts of the wave functions, θ is the unit step function, and the energy of the final state is given by $\epsilon_{k'}=k'^2=\hbar\omega+\epsilon_{n_l,l}$.

Before we continue to present the results obtained for size-dependent photoemission a few general remarks on the method are in order. Experience has shown that the TDLDA is a powerful method for the interpretation of both atomic[14,15] and molecular[16,17] photoabsorption and photoemission spectra. Despite of these successes there are some intrinsic flaws. First of all the use of the LDA, instead of the exact density functional theory, leads to the wrong absolute threshold for photoemission. Second, and highly connected herewith, *all* the thresholds for photoemission from the various occupied levels are wrong due to the absence of relaxation effects in the single-particle states. Out of the general many-particle effects only the linear dielectric effects are built in from the very beginning. Thus, in a more general frame, the TDLDA as used in Refs. 14—17 and in the present work is only able to predict trends but not absolute numbers. It is only for systems with minor relaxation effects that all these flaws are unimportant.

Quite recently, Zangwill and Liberman[18] have shown how to modify the TDLDA (via transition-state orbitals) to (empirically) account for relaxation effects in situations where they are important. The interested reader is referred to their work. In the present context we do not take into account these effects mainly because this work is exploratory in nature. However a first way to mimic these relaxation effects is to change the frequency scale by a constant shift. This is justified because a detailed study within the so-called "ΔSCF theory" shows that the relaxation energy within the valence band is nearly *level independent*,[38] which means that the photoemission spectrum is simply shifted but not distorted upon inclusion of relaxation. With these remarks in mind, we think the TDLDA is a powerful microscopic working scheme to attain *first* realistic insight into the importance of many-particle effects in photoemission from small metal particles (modeled by a KS sphere). Furthermore, since the

method works so well in *both* the case of atoms and molecules[14–17] *and* in the case of a semi-infinite half-space[13,39] there is no reason to doubt the validity of the TDLDA in the range of intermediate particle size. Hence, there remains only the question to answer how spherical real metal clusters of Na or K are. We think that the experimental results of Knight *et al.* on Na and K show clearly that a spherical approximation is *not* so bad in explaining the size-dependent *trends* in the data. Of course this is *not* to say that a dimer looks like a sphere. It simply means that for a large number of particles within the cluster the loosely bound valence electrons mainly feel the spherically averaged potential of a lattice of weak pseudo-ions.

In Fig. 11 we show the photoemission cross section $\sigma(\omega)$ in units of its geometrical value πR^2, for a small sphere of sodium $r_s=4$, corresponding to $N=198$ valence electrons. The frequency is scaled with the frequency of the classical surface plasmon of an $r_s=4$ sphere, $\omega_p/\sqrt{3}=0.2497$ Ry$=3.398$ eV. At the bottom of the figure the threshold energies for photoemission from the various shells occupied in the ground state are marked by arrows. The figure shows $\sigma(\omega)$ at three different levels of approximations. The dashed line is the TDLDA result obtained via (20). The crosses correspond to $\sigma(\omega)$ if in the calculations not the self-consistently obtained potential $V_{\rm SCF}$, Eq. (19), is used, but instead the potential of the classical, local electrodynamics, namely

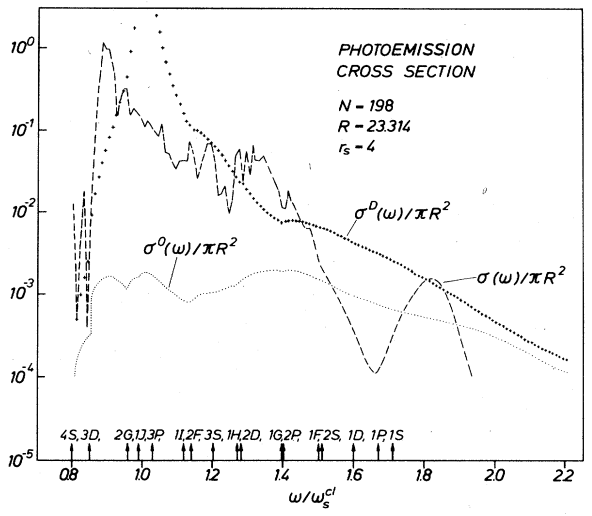

FIG. 11. Photoemission cross section in units of its geometrical value πR^2, at three different levels of approximation, for $N=198$ and $r_s=4$. Dashed line, TDLDA, Eq. (20) of the text; dotted line, bare matrix element result, that means $V_{\rm SCF}(r,\omega)$ is replaced with $V_{\rm ex}=-r$. Crossed line, $V_{\rm SCF}(r,\omega)$ is replaced by the classical Drude potential, Eq. (21) of the text. The most important differences between the TDLDA and the crossed line are as follows: first, the missing volume plasmon peak in the latter, second the red-shifted Mie resonance in the TDLDA, and third the enhanced value of the TDLDA at threshold. The dotted line shows that there are no pronounced features due to pure matrix element effects. At the bottom of the figure, the thresholds for photoemission from the various occupied shells are marked with arrows.

$$V_{\rm cl}(r,\omega)=\begin{cases}-r\left[1-\dfrac{\epsilon(\omega)-1}{\epsilon(\omega)+2}\right], & r<R\\ -r\left[1-\left[\dfrac{R}{r}\right]^3\dfrac{\epsilon(\omega)-1}{\epsilon(\omega)+2}\right], & r>R\ .\end{cases}\tag{21}$$

In this equation, $\epsilon(\omega)$ is the Drude dielectric constant. Finally, the dots correspond to $\sigma(\omega)$ if no screening was present, $V=V_{\rm ex}=-r$. Thus, this curve shows how matrix element effects influence the shape of $\sigma(\omega)$. As expected for loosely bound extended states in a shallow potential there are, generally, no pronounced structures in $\sigma(\omega)$ due to matrix element effects.

On comparing the *shape* of $\sigma(\omega)$ with the corresponding absorption curve, Fig. 4, we see clearly that $\sigma(\omega)$ is not strictly proportional to $\mathrm{Im}\alpha(\omega)$ (as it is very often assumed in phenomenological models of the photoyield[40,41]). The reason for this is simply that for an arbitrary frequency *below* the topmost bound continuum threshold (the $1S$-continuum threshold in Figs. 11–13) the total photoabsorption rate consists of *both* bound-bound *and* bound-continuum transitions, respectively, and only the latter contribute to emission. Nevertheless, there are strong similarities between $\sigma(\omega)$ and $\mathrm{Im}\alpha(\omega)$, even for frequencies ω smaller than the one corresponding to the topmost threshold. The reason for this is that every resonance in $V_{\rm SCF}(r,\omega)$ shows up as a corresponding structure both in $\mathrm{Im}\alpha(\omega)$ and in $\sigma(\omega)$. Hence, the absolute maximum of $\sigma(\omega)$ is at the frequency of surface-plasmon absorption and, even more striking compared to classical electrodynamics, there is a pronounced structure in $\sigma(\omega)$ around ω_p due to the resonant excitation of the volume plasmon. Of course, this structure is missing in the other two curves. At threshold, there is a large enhancement over the bare photoemission rate, whereas at high frequencies all the models approach the same value. The big enhancement at threshold relates to the general fact that, due to the electron-electron interaction, oscillator strength is transferred to the collective poles (at the cost of single pairs). This can be clearly seen by comparing the independent particle response with the response of the interacting particles.[11] In a forthcoming publication it is explicitly shown that this transfer of oscillator strength is strongly dependent on the l value of the general response. Whereas in the dipolar case ($l=1$, the case under discussion in the present paper) the effect is strong, it is nearly negligible for l values in the range of $l=8,9,10$. This is not so surprising because l can be related, via $q=l/R$, to an equivalent wave vector for which a critical value does exist, even for a spherical surface. If l exceeds a critical value l_c, the collective mode starts losing its meaning. Hence, for $l>l_c$ the independent-particle response and the interacting-particle response look very similar.

From these general remarks we see that the enhancement obtained for the present example is, in a certain sense, accidental because the threshold frequency is near the collective frequency. A study of this effect as a function of the r_s value should then reveal general trends in this enhancement mechanism.

In Figs. 12 and 13 the corresponding results for $N=92$

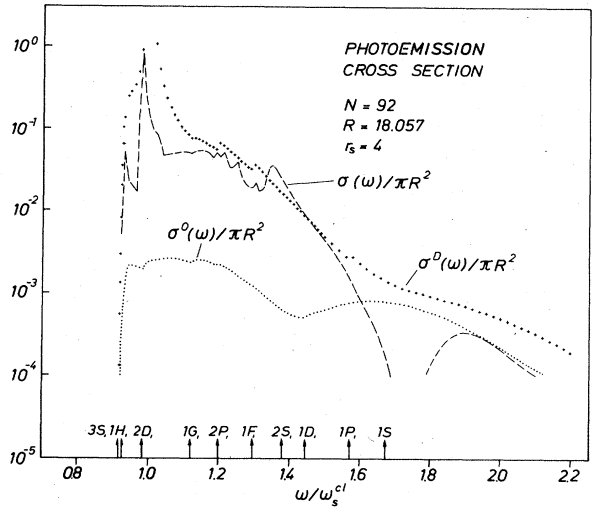

FIG. 12. The same as Fig. 11, but for $N=92$.

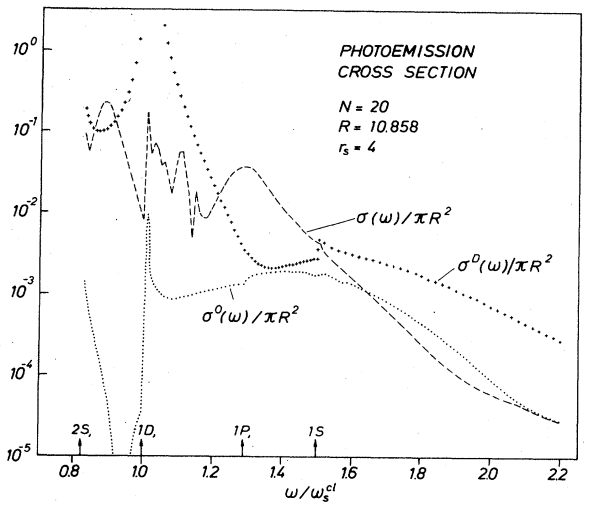

FIG. 13. The same as Fig. 11, but for $N=20$.

and 20, respectively, are shown. These numbers correspond to an uppermost filled shell of the $3s$ and $2s$ type. Generally, all these curves are more or less similar to each other except for details resulting from the different number of levels being filled. The most striking feature in photoemission is the same as in photoabsorption, namely, the vanishing of the volume-plasmon-derived structure if the number of particles decreases. Generally, there are no pronounced features due to matrix element effects except for the near threshold region in the case of $N=20$.

In a recent paper Aers and Inglesfield[42] have argued that the photoyield of a planar metal surface should be similar to the cross section σ^0 in Figs. 11–13. On the basis of this "conjecture," the cross section calculated within the frame of the TDLDA is enhanced near threshold by some orders of magnitude and this would qualitatively explain the experimental findings by Schmidt-Ott *et al.*[35,36]

However, quite recently the same authors[37] have experimentally verified that the photoyield depends *sensitively* on residual gas contamination. Hence, this situation has to be investigated theoretically before a definite conclusion can be drawn on why the yield of a cluster is so drastically enhanced when compared to that of a planar metal surface.

VI. CONCLUSION

A fairly complete study has been presented of the dynamical electronic response properties of small metal spheres within the frame of a completely self-consistent jellium model. Not surprisingly, numerous physical properties deviate from their classical counterparts in a more or less pronounced fashion. There are two simple reasons for this. The smaller the particle is the more important are *both* level quantization effects (so-called quantum size effects) *and* all effects due to the changing surface to volume ratio. A detailed understanding of the various effects can be obtained on the basis of a general competition between the level quantization and the surface diffuseness of the electronic charge. We think that in this way we are able to rationalize Burtscher's experimental observation on the change of the photoyield upon adsorption of rest gas! And a study along this lines is in preparation.

The only larger problem which remains to be solved both for the ground-state and for the response properties is the reintroduction of the lattice of weak pseudo-ions and this problem is presently under study. We think that, with the exception of this lattice effect, all the main ingredients determining the response properties of the electrons in small metal clusters of materials like Na are taken into account in the present study: quantum behavior, self-consistency, nonlocality, and a fairly faithful description of exchange and correlation by the use of the LDA.

ACKNOWLEDGMENTS

The author thanks Professor E. Zeitler for continuing interest and support. Many thanks are due to my colleague J. K. Sass, for many stimulating discussions on the various aspects of surface photoemission. Finally, I would like to express my gratitude to a number of people for discussions and encouragement during the course of this work, especially to P. Apell, J. Inglesfield, W. Knight, B. I. Lundqvist, S. Lundqvist, and M. Sunjić.

[1]For a recent introduction to this rapidly growing field, see for instance, Surf. Sci. **106**, 1 (1981), to be published.

[2]See, for instance, J. Harris, in *The Electronic Structure of Complex Systems, NATO Advanced Study Institute Series,* edited by W. Temmermann and P. Phariseau (Plenum, New York, in press).

[3]W. D. Knight, K. Clemenger, W. A. de Heer, W. A. Saunders, M. Y. Chou, and M. L. Cohen, Phys. Rev. Lett. **52**, 2141 (1984).

[4]W. D. Knight, W. A. de Heer, and K. Clemenger, Solid State

Commun. **53**, 445 (1985).
[5]J. L. Martins, R. Car, and J. Buttet, Surf. Sci. **106**, 265 (1981).
[6]W. Ekardt, Phys. Rev. B **29**, 1558 (1984).
[7]D. E. Beck, Solid State Commun. **49**, 381 (1984).
[8]W. D. Knight, K. Clemengen, W. A. de Heen, and W. A. Saunders, Phys. Rev. B **31**, 2539 (1985).
[9]W. Ekardt, Ber. Bunsenges. Phys. Chem. **88**, 289 (1984); Phys. Rev. Lett. **52**, 1925 (1984); Surf. Sci. (to be published).
[10]D. E. Beck, Phys. Rev. **30**, 6935 (1984).
[11]M. J. Puska, R. M. Nieminen, and M. Manninen, Phys. Rev. B (to be published).
[12]That means we are working within the so-called Rayleigh limit. This is certainly allowed up to the optical region for particles with a diameter of a few tens of angstroms.
[13]P. Feibelmann, Prog. Surf. Sci. **12**, 287 (1982).
[14]A. Zangwill and P. Soven, Phys. Rev. A **21**, 1561 (1980).
[15]A. Zangwill and P. Soven, Phys. Rev. Lett. **45**, 204 (1980).
[16]Z. Levine and P. Soven, Phys. Rev. Lett. **50**, 2074 (1983).
[17]Z. Levine and P. Soven, Phys. Rev. A **29**, 625 (1984).
[18]A. Zangwill and D. A. Libermann, J. Phys. B **17**, L253 (1984).
[19]G. Wendin, J. Phys. B **6**, 42 (1973).
[20]M. Ya. Amusia and N. A. Cherepkov, Case Stud. At. Phys. **5**, 47 (1975).
[21]M. J. Stott and E. Zaremba, Phys. Rev. A **21**, 12 (1980).
[22]M. J. Rice, W. R. Schneider, and S. Strässler, Phys. Rev. B **8**, 474 (1973).
[23]B. B. Dasgupta and R. Fuchs, Phys. Rev. B **24**, 554 (1981).
[24]W. Ekardt, D. B. Tran Thoai, F. Frank, and W. Schulze, Solid State Commun. **46**, 571 (1983).
[25]N. O. Lang and W. Kohn, Phys. Rev. B **7**, 3541 (1973).
[26]S. Andersson, B. N. J. Persson, M. Persson, and N. D. Lang, Phys. Rev. Lett. **52**, 2073 (1984).
[27]R. S. Sorbello, Solid State Commun. **48**, 989 (1983).
[28]D. R. Snider and R. S. Sorbello, Phys. Rev. B **28**, 5702 (1983).
[29]A. A. Lushnikov and A. J. Simonov, Z. Phys. **270**, 17 (1974).
[30]P. Apell and Å. Ljungbert, Phys. Scr. **26**, 113 (1982).
[31]P. Apell and Å. Ljungbert, Solid State Commun. **44**, 1367 (1982).
[32]Å. Ljungbert and P. Apell, Solid State Commun. **46**, 47 (1983).
[33]P. Apell and D. Penn, Phys. Rev. Lett. **50**, 1316 (1983).
[34]S. Lundqvist and P. Apell, J. Phys. (Paris) (to be published).
[35]A. Schmidt-Ott, P. Schurtenberger, and H. C. Siegmann, Phys. Rev. Lett. **45**, 1248 (1980).
[36]H. Burtscher and A. Schmidt-Ott, Phys. Rev. Lett. **48**, 1734 (1982).
[37]H. Burtscher, A. Schmidt-Ott, and H. C. Siegmann, Z. Phys. B **56**, 197 (1984).
[38]W. Ekardt (unpublished).
[39]H. J. Levinson, E. W. Plummer, and P. J. Feibelman, Phys. Rev. Lett. **43**, 952 (1979).
[40]D. R. Penn and R. W. Rendell, Phys. Rev. Lett. **47**, 10 (1981).
[41]D. R. Penn and R. W. Rendell, Phys. Rev. B **26**, 3047 (1982).
[42]G. C. Aers and J. E. Inglesfield, J. Phys. F **13**, 1743 (1983).